

anderes Resultat als bei quantenmechanischer Betrachtung, bei welcher wir das effektive Trägheitsmoment durch Mittelung über  $1/q^2$  gewinnen mußten.

Es wäre jedoch verkehrt, in diesem Ergebnis einen grundsätzlichen Unterschied zwischen klassischer und quantenmechanischer Betrachtung zu sehen. Um das zu erkennen, haben wir nur zu bemerken, daß das quantenmechanische Vorgehen nicht demjenigen in der obigen Versuchsreihe entspricht. Quantenmechanisch hatten wir vorausgesetzt, daß die Energiestufen der inneren Bewegung große Abstände aufweisen gegenüber der durch die Rotation hinzutretenden Störenergie, so daß der innere Zustand durch die Rotation nicht wesentlich gestört wird. Eine solche Annahme entspricht auf der klassischen Seite einem Vorgehen, bei welchem der zunächst rotationsfreie Zustand durch eine adiabatische Einwirkung in Drehung versetzt wird. Das würde also bedeuten, daß wir ein sehr kleines, kon-

stantes Drehmoment über Zeiten hinweg wirken lassen, die groß sind gegen die radiale Schwingungsdauer des Systems, und zwar so, daß das Produkt  $M \cdot t$  immer noch klein bleibt. In diesem Fall liefert die Integration für  $1/\Theta_{\text{eff}}$ , wie man sich leicht – etwa durch partielle Integration – überzeugt, nichts anderes als den Zeitmittelwert von  $1/\mu q^2$ , wobei es auch hier genügt, den Zeitmittelwert über eine einzige Schwingungsdauer zu erstrecken.

Man erkennt also, daß bei entsprechender klassischer Behandlung das effektive Trägheitsmoment in analoger Weise zu gewinnen ist wie in der Quantenmechanik, wobei nur an Stelle des Erwartungswertes der zeitliche Mittelwert zu nehmen ist. Auch in diesem Fall wird natürlich  $\Theta_{\text{eff}}$  stets kleiner als der Mittelwert  $\overline{\mu q^2}$ . Die Überlegungen unseres Abschnitts 7 über das Verhältnis der beiden Größen lassen sich auf klassische Gebilde in ganz analoger Weise übertragen.

## Direct Photodisintegration of $^9\text{Be}$ in the Low and Sub-Giant Resonance Energy Region

TERJE AURDAL

Institut für Theoretische Physik der Universität Tübingen

(Z. Naturforsch. **24 a**, 1188–1195 [1969]; received 16 April 1969)

Photodisintegration cross sections for the reaction  $^9\text{Be}(\gamma, n)^8\text{Be}$  with photonenergies varied from threshold to about 17 MeV are calculated. As nuclear model is assumed a single particle shell model where the valence neutron outside the  $^8\text{Be}$  core is feeling a spherical field. The core state is assumed to be a mixture of the ground ( $0^+$ ) and the first excited ( $2^+$ ) state of the  $^8\text{Be}$  nucleus. The total cross sections are splitted up according to the different contributing reaction channels. The radial wave functions in initial as well as final states are of the Saxon-Woods type.

Photodisintegration of  $^9\text{Be}$  has during the last years been object to detailed research both experimentally<sup>1–4</sup> as well as theoretically<sup>5–8</sup>. In the region from threshold up to about 6 MeV the experimental  $(\gamma, n)$  cross section curve shows three pronounced maxima. The first slightly over the thresh-

old energy, the second at about 3 MeV and the third at about 4.6 MeV. There is also a weak but observable maximum at 2.4 MeV. The neutron angular distribution from the threshold- and the 4.6 MeV-peak appear to be isotropic, while the 3 MeV excitation maximum gives anisotropic distribution.

Reprint request to T. Aurdal, Institut für Theoretische Physik der Universität Tübingen, D-7400 Tübingen, Gartenstraße 47.

<sup>1</sup> B. L. BERMAN, R. L. VAN HEMERT, and C. D. BOWMAN, Phys. Rev. **163**, 958 [1967].

<sup>2</sup> B. HAMERMESH and C. KIMBALL, Phys. Rev. **90**, 1063 [1953]. — W. JOHN and J. M. PROSSER, Phys. Rev. **127**, 231 [1962].

<sup>3</sup> R. NATHANS and J. HALPERN, Phys. Rev. **92**, 940 [1953]. — R. D. EDGE, Nucl. Phys. **2**, 485 [1956/57]. — S. COSTA, L. PASQUALINI, G. PIRAGINO, and L. ROASIO, Nuovo Cimento **42 B**, 306 [1966].

<sup>4</sup> M. J. JAKOBSON, Phys. Rev. **123**, 229 [1961].

<sup>5</sup> E. GUTH and C. J. MULLIN, Phys. Rev. **74**, 833 [1948]; **76**, 234 [1949].

<sup>6</sup> N. C. FRANCIS, D. T. GOLDMAN, and E. GUTH, Phys. Rev. **120**, 2175 [1960].

<sup>7</sup> J. S. BLAIR, Phys. Rev. **123**, 2151 [1961].

<sup>8</sup> S. BOFFI, J. SAWICKI, and E. SCACCIATELLI, Nuovo Cimento **52 B**, 210, 244 [1967].



Dieses Werk wurde im Jahr 2013 vom Verlag Zeitschrift für Naturforschung in Zusammenarbeit mit der Max-Planck-Gesellschaft zur Förderung der Wissenschaften e.V. digitalisiert und unter folgender Lizenz veröffentlicht: Creative Commons Namensnennung-Keine Bearbeitung 3.0 Deutschland Lizenz.

Zum 01.01.2015 ist eine Anpassung der Lizenzbedingungen (Entfall der Creative Commons Lizenzbedingung „Keine Bearbeitung“) beabsichtigt, um eine Nachnutzung auch im Rahmen zukünftiger wissenschaftlicher Nutzungsformen zu ermöglichen.

This work has been digitalized and published in 2013 by Verlag Zeitschrift für Naturforschung in cooperation with the Max Planck Society for the Advancement of Science under a Creative Commons Attribution-NoDerivs 3.0 Germany License.

On 01.01.2015 it is planned to change the License Conditions (the removal of the Creative Commons License condition “no derivative works”). This is to allow reuse in the area of future scientific usage.

From the position and parity of the energy levels<sup>9</sup> there is reason to believe that:

a) the threshold- and the 3 MeV-peak is due to E1 transitions with the neutron emitted as S wave and D wave, respectively.

b) the 4.6 MeV-peak is probably E1 transitions with the neutron emitted as a D wave or as a S wave, with the residual nucleus left in its first ( $2^+$ ) excited state. The area  $\int \sigma_\gamma dE_\gamma$  attributed to the 4.6 MeV-peak is about two times that of the threshold peak.

c) the 2.4 MeV-peak can be explained by M1 or E2 transitions only.

In the intermediate energy region the experiments<sup>3</sup> indicate total  $(\gamma, n)$  cross sections of the typical Pygmy resonance structure. Detailed theoretical analysis of the  $(\gamma, n)$  cross sections in this energy region is so far, not reported.

Most of the low-energy photodisintegration calculations are based on a spherical shell-model where the  ${}^8\text{Be}$  nucleus plays the part of an inert core without internal structure. Within the frame of this model there are reported calculations accomplished with a potential of the Saxon-Woods type, but taking account of S wave emission of the neutron only<sup>6</sup>. To get reasonable fitting to the experimental cross sections one had to use an unrealistic large diffuseness parameter in the final state. This can, as shown by BLAIR<sup>7</sup>, to a certain degree be avoided by introducing reduced widths of the reaction channels. A reduction factor for the S wave emission of about 0.60 calculated by BLAIR, combined with a not too large diffuseness parameter, gives reasonable fitting to the threshold cross section peak.

A more sophisticated model for the excitation mode of the  ${}^9\text{Be}$  nucleus is introduced by KUNZ, HENLEY and BLAIR<sup>10</sup>, and in a simplified version by KOWALSKA<sup>11</sup>. In these models the core deformation or the internal core structure of two  $\alpha$ -particles is taken into account. The essential feature of the simplified version, the KOWALSKA model, is the final state approximation where the excited nucleon is feeling a spherical field while the residual nucleus can be left in a rotational excited state corresponding to an intrinsic deformation.

A still more sophisticated model of the  ${}^9\text{Be}$  nucleus is the  $\alpha$ -particle model developed by HIURA and SHIMODAYA<sup>12</sup>, but numerical calculations are lacking.

BOFFI et al.<sup>8</sup> have calculated cross sections with initial state wavefunctions of the Bohr, Mottelson, Nilsson type assuming strong nuclear deformation. The final states were vector products of the single-particle wavefunctions of the valence neutron in the continuum with the wavefunction of a core-state possibly with rotational excitation. The continuum single-particle wavefunctions were approximated by those corresponding to an average spherical field.

The numerical analysis was limited to a square well of common range radius  $r_0$  and of well depths  $V_{ijL}$  depending on the state quantum numbers. The numerical values of  $V_{ijL}$  were fixed fitting the energies of the peaks of the total cross section  $\sigma_T$  corresponding to the individual states  $(l, j, L)$ . The energy  $E_n$  of the outgoing neutron was fixed by  $E_n = E_\gamma - |E_B| - E_{\text{rot}}^L$ , where  $E_\gamma$  is the photonenergy,  $E_B$  the neutron binding energy in the ground state and  $E_{\text{rot}}^L$  is the possible rotational energy of the core in the final state. The calculated cross sections were in agreement with experimental data of JAKOBSON<sup>4</sup>.

In the present work the wavefunctions are taken to be totally antisymmetrized shell-model functions where the extra valence neutron is isolated with the coefficients of fractional parentage technique. This expansion of the initial state wave function will in addition to a  $L=0$  state also make possible a  $L=2$  state of the core, which is similar to the rotational state in the Kowalska model. The final state wavefunction is single-particle wavefunctions of the valence neutron in continuum, vector coupled to core states which are assumed to be a mixture of  $L=0$  and  $L=2$  states. The weight factors of these two core states are assumed equal to the weightfactors (the fractional parentage coefficients) of the corresponding initial states. In the final states there are also assumed coupling between the angular momenta of the outgoing neutron and of the core.

In the following paragraph the necessary mathematical formulae are developed and the general equation of the  $(\gamma, n)$  cross section is established.

<sup>9</sup> T. LAURITZEN and F. AJZENBERG-SELOVE, Nucl. Phys. **78**, 1 [1966].

<sup>10</sup> J. S. BLAIR and E. M. HENLEY, Phys. Rev. **112**, 2029 [1958]. — E. M. HENLEY and P. D. KUNZ, Phys. Rev. **118**, 248 [1960]. — P. D. KUNZ, Ann. Phys. New York **11**, 275 [1960].

<sup>11</sup> A. KOWALSKA, Acta Phys. Polon. **21**, 583 [1962].

<sup>12</sup> J. HIURA and I. SHIMODAYA, Progr. Theor. Phys. **30**, 585 [1963].

The cross sections are classified according to the quantum numbers  $(l, L, J)$  which are the orbital angular momentum of the outgoing neutron, the total angular momentum of the residual nucleus and the channel spin, respectively. All numerical calculations are accomplished with Saxon-Woods radial wavefunctions in both initial- and final-states<sup>13</sup>. In Section 2 the obtained results which are shown in Figs. 2–4 are discussed. Section 3 is devoted to a short general discussion and conclusions.

### 1. General Theory

In the mass region  $4 < A \leq 16$  it is common practice to assume a ground state configuration which is principally  $(1s)^4(1p)^{A-4}$ , with some configuration interactions treated as higher order corrections. The ground state configuration of  ${}^9\text{Be}$  is due to this  $(1s)^4(1p)^5$ , within the first order approximation. We further accept  $LS$  coupled functions as basis for our wavefunctions.

In the low-energy region the inner  $(1s)^4$  shell can without much error, be considered as an inert core and be neglected. The construction of a totally antisymmetric ground-state wavefunction of  ${}^9\text{Be}$  reduces then to a construction of the possible antisymmetric states of the five  $1p$  nucleons. The resulting state-functions belonging to four different symmetry classes, can be classified according to their orbital partition quantum numbers and the corresponding Young diagrams.

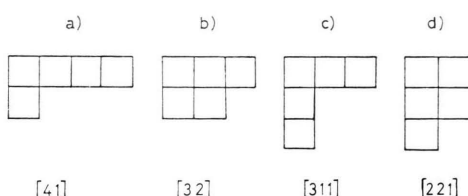


Fig. 1. Young diagrams describing possible symmetry classes of the ground state  ${}^9\text{Be}$  wavefunction.

The inner  $(1s)^4$  shell may be added as an extra 4-row on top of the diagrams. Of these four possible Young diagrams the one with the highest orbital symmetry i. e. a) is the most important, and we accept this as the representation to which our ground-state wavefunction belongs.

The ground-state wavefunction of  ${}^9\text{Be}$  is therefore described by the following quantum numbers, all having their usual significance.

$$\Psi[(1s)^4(1p)^5[\lambda] = [441],$$

$$S = \frac{1}{2}, \quad T = \frac{1}{2}, \quad L = 1, \quad J^\pi = \frac{3}{2}^-. \quad (1)$$

The inner  $(1s)^4$  shell is here referred to only for completeness.

In the following we shall develop the mathematical formulae in order to calculate electric dipole  $(\gamma, n)$  cross sections on  ${}^9\text{Be}$ . We assume as nuclear model a core consisting of two  $\alpha$ -like particles and an outer valence nucleon, and further that  $E1$  transitions of the valence nucleon represent the only contributions to the cross section in the low-energy region.

Using the method of fractional parentage coefficients, it is possible to decouple the statefunction (1) and isolate one nucleon in a way that it may be considered as a valence nucleon. However, this decoupling is in general not straightforward, and in the case of  ${}^9\text{Be}$  there is more than one resulting state-function of an allowed symmetry.

Generally the partition quantum number characterizes the irreducible representation of the group  $S_n$ , where  $n$  is the total number of nucleons involved. Such a partition is conveniently described by a Young diagram. An irreducible representation  $[\lambda]$  of  $S_n$  is in general reducible with respect to the subgroup  $S_{n-1}$ . The number and type  $[\lambda']$  of representations of  $S_{n-1}$  into which the representation  $[\lambda]$  reduces, is determined by the number and type of allowed Young diagrams obtained from that of  $[\lambda]$  by removing one square. The representations of  $S_{n-1}$  are in turn themselves in general reducible with respect to the subgroup  $S_{n-2}$  and so on, until one arrives at the one-dimensional representation  $[1]$  of  $S_1$ . A function is then characterized by the string of representations  $S_n \supset S_{n-1} \supset S_{n-2} \supset \dots \supset S_2 \supset S_1$  to which it belongs.

Such a characterization of the function spreading out the representation  $[\lambda]$  of  $S_n$  may be conveniently described by a Yamanouchi symbol

$$(r) = (r_n r_{n-1} \dots r_1 = 1)$$

which in a unique way describes the string of representations  $S_n \supset \dots \supset S_1$ .

The different ways of decoupling one nucleon will then be characterized by different strings of representations  $S_n \supset \dots \supset S_1$ , or equivalently by different Yamanouchi symbols.

<sup>13</sup> T. AURDAL, Thesis, University of Bergen 1968, unpublished. — T. AURDAL, Z. Naturforsch. **24a**, 461 [1969].

The accepted ground-state wavefunction of  ${}^9\text{Be}$  belongs to the irreducible representation [41]. The wavefunction may, by a method outlined by JAHN<sup>14</sup>, be written as a product of purely orbital functions and purely spin-charge functions allowing the fractional parentage coefficients of the different parts to be calculated independently. The spin-charge functions belong to the adjoint representation  $[\tilde{\lambda}]$  of the same dimension  $n_{\lambda}$ , as the representation  $[\lambda]$  of the orbital functions. The wavefunction of  ${}^9\text{B}$  is written as:

$$\begin{aligned} & \Psi(p^5[41] T S L M_T M_S M_L | 5 4 3 2 1) \\ &= \frac{1}{\sqrt{n_{\lambda}}} \sum_{(r)=1}^{\gamma_u} \Phi(p^5[41] L M_L | r_5 r_4 r_3 r_2 r_1) \\ & \cdot \Gamma(\gamma^5[\tilde{4}\tilde{1}] T S M_T M_S | \tilde{r}_5 \dots \tilde{r}_1). \end{aligned} \quad (2)$$

The summation extends over all the  $n_{\lambda}$  possible Yamanouchi symbols associated with the partition [41].

After expanding the orbital- and spin-charge wavefunctions using their corresponding fractional parentage coefficients, Eq. (2) may be written:

$$\begin{aligned} & \Psi(p^5[41] T S L J M_T M_S M_L M_J | 5 4 3 2 1) \\ &= \frac{1}{\sqrt{n_{\lambda}}} \sum_{(r)=1}^{n_{\lambda}} \sum_{\substack{L'S'T' \\ \text{magn}}} \{ \langle p^5[41] L | p^4[\lambda'] L' \rangle \langle \gamma^5[\tilde{4}\tilde{1}] T S | \gamma^4[\tilde{\lambda}'] T' S' \rangle (L M_L S M_S | L S J M_J) \\ & \times \Phi(p^4[\lambda'] L' (r_4 \dots r_1), p_5, L M_L) \Gamma(\gamma^4[\lambda'] T' S' (\tilde{r}_4 \dots \tilde{r}_1), \gamma_5, T S M_T M_S) \}. \end{aligned} \quad (3)$$

The values of  $[\lambda']$  and  $[\tilde{\lambda}']$  occurring vary with  $(r)$ . We have also coupled the orbital- and spin-angular momentum to a total angular momentum  $J$ .

Eq. (3) may also be written:

$$\begin{aligned} & \Psi(p^5[41] T S L J M_T M_S M_L M_J | 5 4 3 2 1) \\ &= \frac{1}{\sqrt{n_{\lambda}}} \sum_{[\lambda']} \sum_{\substack{L'S'T' \\ \text{magn}}} \{ \langle p^5[41] L | p^4[\lambda'] L' \rangle \langle \gamma^5[\tilde{4}\tilde{1}] T S | \gamma^4[\tilde{\lambda}'] T' S' \rangle (L M_L S M_J | L S J M_S) \\ & \times \sum_{(r')=1}^{n_{\lambda}'} \Phi(p^4[\lambda'] L' (r_4 \dots r_1), p_5, L M_L) \Gamma(\gamma^4[\tilde{\lambda}'] T' S' (\tilde{r}_4 \dots \tilde{r}_1), \gamma_5, T S M_T M_S) \} \end{aligned} \quad (4)$$

where the summation over  $[\lambda']$  corresponds to those diagrams for 4 particles, which may be obtained from the Young diagram [41] for 5 particles by removing one square in an allowed manner. The summation over  $(r')$  covers all the allowed Yamanouchi symbols of  $[\lambda']$ .

The orbital part and the spin-charge part of the wave-function can independently be separated into products of core- and valence nucleon-wavefunctions by ordinary vector-coupling coefficients.

We write:

$$\begin{aligned} & \Phi(p^4[\lambda'] L' (r_4 \dots r_1), p_5, L M_L) \\ &= \sum_{\text{magn}} \{ (L' M_L' 1 m_l | L' 1 L M_L) \cdot \Phi_c(p^4[\lambda'] L' (r_4 \dots r_1), M_L') \cdot \Phi_{v.n.}(p_5[1], 1 m_l) \} \end{aligned} \quad (5)$$

$$\begin{aligned} \text{and} \quad & \Gamma(\gamma^4[\tilde{\lambda}'] T' S' (\tilde{r}_4 \dots \tilde{r}_1), \gamma_5, T S M_T M_S) = \sum_{\text{magn}} \{ (T' M_T' \tfrac{1}{2} m_{\tau} | T' \tfrac{1}{2} T M_T) \\ & \times (S' M_S' \tfrac{1}{2} m_s | S' \tfrac{1}{2} S M_S) \cdot \Gamma_c(\gamma^4[\lambda'] T' M_T' S' M_S') \cdot \Gamma_{v.n.}(\gamma_5 \tfrac{1}{2} m_{\tau}) \cdot \Gamma_{v.n.}(\gamma_5 \tfrac{1}{2} m_s) \}. \end{aligned} \quad (6)$$

Substituting Eqs. (5) and (6) in Eq. (4), inserting also the right quantum numbers, it may be written:

$$\begin{aligned} & \Psi(p^5[41] \tfrac{1}{2} \tfrac{1}{2} 1 \tfrac{3}{2} M_T M_S M_L M_J | 5 4 3 2 1) \\ &= \frac{1}{\sqrt{n_{\lambda}}} \sum_{[\lambda']} \sum_{L'S'T'} \{ \langle p^5[41] 1 | p^4[\lambda'] L' \rangle \langle \gamma^5[\tilde{4}\tilde{1}] \tfrac{1}{2} \tfrac{1}{2} | \gamma^4[\tilde{\lambda}'] T' S' \rangle (1 M_L \tfrac{1}{2} M_S | 1 \tfrac{1}{2} \tfrac{3}{2} M_J) \\ & \times (L' M_L' 1 m_l | L' 1 L M_L) (T' M_T' \tfrac{1}{2} m_{\tau} | T' \tfrac{1}{2} \tfrac{1}{2} M_T) (S' M_S' \tfrac{1}{2} m_s | S' \tfrac{1}{2} \tfrac{3}{2} M_S) \\ & \times \sum_{(r')=1}^{n_{\lambda}'} \Phi_c(p^4[\lambda'] L' (r_4 \dots r_1) M_L') \cdot \Gamma_c(\gamma^4[\tilde{\lambda}'] T' M_T' S' M_S') \\ & \cdot \Phi_{v.n.}(p_5[1] 1 m_l) \cdot \Gamma_{v.n.}(\gamma_5 \tfrac{1}{2} m_{\tau}) \cdot \Gamma_{v.n.}(\gamma_5 \tfrac{1}{2} m_s) \}. \end{aligned} \quad (7)$$

<sup>14</sup> H. A. JAHN and H. VAN WIERINGEN, Proc. Roy. Soc. London A **209**, 502 [1951].

From the partition [41] the summation in Eq. (3) extends over the following possible Yamanouchi symbols

$$\begin{array}{ll} \text{a)} & \text{b)} \\ (2\ 1\ 1\ 1\ 1) = \begin{pmatrix} 1\ 2\ 3\ 4 \\ 5 \end{pmatrix} & (1\ 2\ 1\ 1\ 1) = \begin{pmatrix} 1\ 2\ 3\ 5 \\ 4 \end{pmatrix} \\ \text{c)} & \text{d)} \\ (1\ 1\ 2\ 1\ 1) = \begin{pmatrix} 1\ 2\ 4\ 5 \\ 3 \end{pmatrix} & (1\ 1\ 1\ 2\ 1) = \begin{pmatrix} 1\ 3\ 4\ 5 \\ 2 \end{pmatrix} \end{array}$$

These are in the same order, belonging to the following strings of representations.

$$\begin{array}{ll} \text{a)} & [41], \quad [4], \quad [3], \quad [2], \quad [1] \\ \text{b)} & [41], \quad [31], \quad [3], \quad [2], \quad [1] \\ \text{c)} & [41], \quad [31], \quad [21], \quad [2], \quad [1] \\ \text{d)} & [41], \quad [31], \quad [21], \quad [11], \quad [1] \end{array} \quad (8\ b)$$

The ground-state  ${}^9\text{Be}$  wavefunction may be written:

$$\begin{aligned} \Psi_{\text{g.s.}}^i({}^9\text{Be}) = \frac{1}{2} \sum_{L'} \{ p^5[41] \ 1 \mid p^4[4] \ L' \} \cdot (1\ M_L \ \frac{1}{2} \ M_S \mid 1\ \frac{1}{2} \ \frac{3}{2} \ M_J) (L' \ M_L' \ 1\ m_l \mid L' \ 1\ 1\ M_L) \\ \times \Phi_c^i(p^4[4] \ L' (1111) \ M_L') \cdot \Phi_c^i(\gamma^4[1111] \ 0000) \cdot \Phi_{\text{v.n.}}^i(p_5 \ 1\ m_l) \cdot \Phi_{\text{v.n.}}^i(\gamma_5 \ \frac{1}{2} \ m_\tau) \cdot \Phi_{\text{v.n.}}^i(\gamma_5 \ \frac{1}{2} \ m_s) \}. \end{aligned} \quad (9)$$

The summation over  $L'$  extends over the values  $L' = 0$  and  $L' = 2$ . The corresponding f.p.c. are tabulated<sup>14</sup>.

In order to construct a reasonable final state wavefunction, we assume that after emission of the valence nucleon the core can be left in an excited state. We therefore construct our final state wavefunction as vector products of the continuum states of the valence nucleon with the core states which is assumed to be a mixture of  $L'' = 0$  and  $L'' = 2$  states. The two core states are given the same weightfactors as the corresponding initial states.

$$\begin{aligned} \Psi^f({}^9\text{Be}) = \sum_{L''} \{ \alpha_{L''} (L'' \ M_L'' \ l' \ m_l' \mid L'' \ l' \ L \ \bar{M}_L) (L \ \bar{M}_L \ \frac{1}{2} \ m_s' \mid L \ \frac{1}{2} \ J \ M_J) \\ \times \Psi_c^f([4] \ L'' \ M_L'') \cdot \Psi_c^f([\tilde{4}] \ T=0, S=0) \cdot \Psi_{\text{v.n.}}^f(l' \ m_l') \cdot \Psi_{\text{v.n.}}^f(\frac{1}{2} \ m_s') \cdot \Psi_{\text{v.n.}}^f(\frac{1}{2} \ m_\tau) \}. \end{aligned} \quad (10)$$

The spin- and charge-Clebsch-Gordan coefficients are trivial and therefore omitted.

The total orbital angular momentum and the total spin are coupled to give a total angular momentum or channel spin, of the system in the final state.

The electric dipole cross sections are given by the equation

$$\sigma(E1) = K \left| \langle \Psi^f \mid \sum_{k=1}^A \varepsilon_k r_k Y_1^1(\vartheta_k, \varphi_k) \mid \Psi_{\text{g.s.}}^i \rangle \right|^2 \quad (11)$$

where the quantity  $K$  depends on the reduced nucleon mass, the density of final states and the wave number of the outgoing nucleon<sup>13</sup>.

Inserting the expressions (9) and (10) for the initial and final states, respectively, Eq. (11) may be written

$$\begin{aligned} \sigma(E1) = K \left| \sum_{\substack{L'' L' J_f \\ \text{magn}}} \Theta_{L' L''}^J \langle \Psi_c^f([4] \ L'' \ M_L'') \cdot \Psi_c^f([\tilde{4}] \ T=0, S=0) \cdot \Psi_{\text{v.n.}}^f(l' \ m_l') \cdot \Psi_{\text{v.n.}}^f(\frac{1}{2} \ m_\tau) \cdot \Psi_{\text{v.n.}}^f(\frac{1}{2} \ m_s') \mid \right. \\ \times \sum_{k=1}^A \varepsilon_k r_k Y_1^1(\vartheta_k, \varphi_k) \mid \cdot \Phi_c^i(p^4[4] \ L' (1111) \ M_L') \cdot \Phi_c^i(\gamma^4[1111] \ 0000) \\ \left. \cdot \Phi_{\text{v.n.}}^i(\frac{1}{2} \ m_\tau) \cdot \Phi_{\text{v.n.}}^i(1\ m_l) \cdot \Phi_{\text{v.n.}}^i(\frac{1}{2} \ m_s) \rangle \right|^2 \end{aligned} \quad (12)$$

When decoupling one nucleon from the [41] representation we easily verify that the representation string a) conserves a core-structure of two  $\alpha$ -particles [the  $(1s)^4$  shell included], while b), c) and d) correspond to a break up of this  $\alpha$ -structure. Since in our  ${}^9\text{Be}$  model we want to retain a core-structure of two  $\alpha$ -particles, we disregard the states corresponding to the representations b), c) and d). This will fix the diagrams  $[\lambda']$  and  $[\lambda'']$  and the summation over  $(r')$  in Eq. (7) reduces to one term.

With this choice of representation of the statefunctions the spin-charge fractional parentage coefficients as well as the spin-charge Clebsch-Gordan coefficients are trivial and may be omitted.



where

$$\begin{aligned} \Theta_{L'L''}^J &= \frac{1}{2} \alpha_{L''} \langle p^5[41] 1 | p^4[4] L' \rangle (L'' M_L'' l' m_l' | L'' l' L \bar{M}_L) \\ &\times (L \bar{M}_L \frac{1}{2} m_s' | L \frac{1}{2} J M_J) \cdot (1 M_L \frac{1}{2} m_s | 1 \frac{1}{2} \frac{3}{2} M_J) \cdot (L' M_L' 1 m_l | L' 1 1 M_L). \end{aligned}$$

The electric dipole operator is depending on the nucleon-charge coordinates only through the effective charge. Disregarding the Coulomb barrier Eq. (12) may be attributed to the photo-proton as well as to the photo-neutron cross sections. We may specify Eq. (12) to the neutron case by setting  $m_\tau = \div \frac{1}{2}$ , but the spin-charge functions of the core as well as of the valence neutron will give by summing over the possible states, Kronecker-deltas and can therefore be omitted. We write:

$$\begin{aligned} \sigma(E1) &= K \left| \sum_{\substack{L'L''J \\ \text{mag}}} \Theta_{L'L''}^J \langle \Psi_c^i([4] L'' M_L'') \cdot \Psi_{v.n.}^f(l' m_l') \rangle \right. \\ &\quad \left. \times \sum_{k=1}^A \varepsilon_k r_k Y_1^1(\vartheta_k, \varphi_k) | \Phi_c^i(p^4[4] L' M_L') \cdot \Phi_{v.n.}^1(1 m_l) \rangle \right|^2. \end{aligned} \quad (13)$$

Using standard Racah algebra Eq. (13) can be easily reduced and the different contributions to the total cross sections classified according to the channel spin. Contraction of Eq. (13) results in equations of the type.

$$\sigma_J(E1) = K \sum_{\mu=0,2} \{ (A_\mu \alpha_1^4 + B_\mu \alpha_1^2 \alpha_2^2 + C_\mu \alpha_2^4) \cdot I_\mu^2 \} \quad (14)$$

where  $J$  the channel spin, can have the values  $J = \frac{1}{2}, \frac{3}{2}, \frac{5}{2}$ . The quantities  $A_\mu$ ,  $B_\mu$  and  $C_\mu$  ( $\mu = 0, 2$ ) are constants, not necessarily all nonzero for all possible  $J$  values. The factors  $\alpha_1$  and  $\alpha_2$  are the fractional parentage coefficients for  $L' = 0$  and  $L' = 2$ , respectively. Considering them as parameters gives us the possibility to attribute to the different reaction channels varying widths.

The radial integrals for the different  $l$  values of the outgoing nucleon are defined by

$$I_\mu = \int_0^\infty R_{l_1}(r) \cdot R_{l_2=\mu}(r) \cdot r^3 dr, \quad \mu = 0, 2 \quad (15)$$

where  $R_l(r)$ , the radial functions, are generated in a Saxon-Woods potential.

## 2. Results

It is attempted in the present work to account for the data of JAKOBSON<sup>4</sup> in the energy range from threshold to 5 MeV, and the data of NATHANS and HALPERN<sup>3</sup> and COSTA et al.<sup>3</sup> in the region from 5 MeV to about 17 MeV. The low energy NATHANS/HALPERN data are inconsistent with the recent data of JAKOBSON, hence the two data sets are matched at 5 MeV where they are in agreement.

During the calculations the initial state potential is characterized by the parameters:

a common radius parameter  $r_0 = 1.35$  fm in all states independent of their quantum numbers, a diffuseness parameter  $0.6 \text{ fm} \leq a \leq 0.7$  fm depending on the state quantum numbers and a potential depth  $V = 35 - 40$  MeV fixed by the binding energy of the valence neutron.

Reflecting the fact that the  ${}^8\text{Be}$  nucleus is a weakly bound structure, the final state parameters are given the following values. In the low energy region the radius parameter is kept constant whilst the diffuseness parameter  $a_0$  is enlarged 0.20 fm relative to the initial state. In the energy regions where the  $2^+$  core state is important, the radius parameter is increased 0.1 fm whilst  $a_0$  is made only slightly dependent on the state quantum numbers. The potential depth is varied with the quantum numbers of the states, corresponding to their different energies. In addition the potential depth in the neutron D states is increased relative to a neighbouring neutron S state simulating the effect of a spin-orbit term.

As a test of the correctness of the parameters, phase shifts of elastic neutron scattering on  ${}^8\text{Be}$  are calculated, Fig. 4. These are compared with phase shifts calculated by CORMAN et al.<sup>15</sup> from the same potential and with parameter values given in order to fit experimental polarization data of the photo-neutrons from  ${}^9\text{Be}$ . The present calculations are in encouraging agreement with CORMAN's results.

The different states as well as their contributions to the total cross section, are classified according to the quantum numbers  $(l, L, J)$  which are the orbital

<sup>15</sup> E. G. CORMAN, R. W. JEWELL, W. JOHN, J. E. SHERWOOD, and D. WHITE, Phys. Letters **10**, 116 [1964].

angular momentum of the valence neutron, the orbital angular momentum of the core and the channel spin, respectively. The results of the calculations which are shown in Fig. 2 and 3, can be summed up as follows.

*The 1.7 MeV resonance:* This resonance close to the threshold energy of the  $(\gamma, n)$  reaction, can be fully explained as E1 transitions between the states.

$$(l=1, L=0, J^\pi = \frac{3}{2}^-) \rightarrow (l=0, L=0, J^\pi = \frac{1}{2}^+). \quad (1)$$

The neutron is emitted as a S wave in agreement with the reported isotropic angular neutron distribution in this energy region. The maximum of the peak is corresponding to a broad  $J^\pi = \frac{1}{2}^+$  level at 1.67 MeV.

*The 2.4 MeV resonance:* A maximum in the  $(\gamma, n)$  cross section at this energy is not found, in agreement with the assumption that this is due to E2 or M1 transitions to a negative parity, spin  $\frac{5}{2}$  level at 2.43 MeV.

*The 2.95 MeV resonance:* The peak in the cross sections with maximum at this energy can be explained as E1 transitions between the states.

$$(l=1, L=0, J^\pi = \frac{3}{2}^-) \rightarrow (l=2, L=0, J^\pi = \frac{5}{2}^+). \quad (2)$$

The resulting state found to be an almost pure  $\frac{5}{2}^+$  state, is in good agreement with the reported  $\frac{5}{2}^+$  level at 3.03 MeV.

The broad minimum beyond the 2.95 MeV resonance may be explained by E1 transitions between the states

$$(l=1, L=0, J^\pi = \frac{3}{2}^-) \rightarrow (l=2, L=0, J^\pi = \frac{3}{2}^+). \quad (3)$$

This is either due to transitions to a yet unresolved level at about 4 MeV like that found in  $^9\text{Be}$  at 4.05 MeV, or transitions to the very broad  $(\frac{3}{2}^+, \frac{5}{2}^+)$  level at 4.7 MeV.

*The 4.6 MeV resonance:* The neutron angular distribution corresponding to the maximum in the total cross section at 4.6 MeV is reported to be dominantly isotropic. This excitation maximum should therefore be attributed to S wave emission of the valence neutron.

Our ground state  $^9\text{Be}$  wavefunction consists of two terms. One where the valence neutron state is coupled to the  $L^\pi = 0^+$  state of the  $^8\text{Be}$  core, and one where it is coupled to the  $L^\pi = 2^+$  core state. Both terms are describing the same nuclear system with the same total energy, the nucleons are only rearranged. The excitation energy of the  $2^+$  core state is 2.90 MeV, and to a good approximation, the va-

lence neutron coupled to this state is tighter bound by the same amount of energy. The binding energy of the valence neutron in the state  $(l=1, L=2, J^\pi = \frac{3}{2}^-)$  is therefore assumed to be

$$E_B = (1.665 + 2.90) \text{ MeV} = 4.565 \text{ MeV}.$$

The 4.6 MeV resonance can in this way be explained as E1 transitions between the states

$$(l=1, L=2, J^\pi = \frac{3}{2}^-) \rightarrow (l=0, L=2, J^\pi = \frac{3}{2}^+).$$

and

$$(l=1, L=2, J^\pi = \frac{3}{2}^-) \rightarrow (l=0, L=2, J^\pi = \frac{5}{2}^+). \quad (4)$$

with the  $\frac{5}{2}^+$  state giving a slightly greater contribution to the S wave neutron cross section than the  $\frac{3}{2}^+$  state. As seen from Fig. 2 the 4.6 MeV resonance is not pure S wave cross sections but is mixed with D wave emission from other  $(\frac{3}{2}^+, \frac{5}{2}^+)$  states. The maximum of the resonance is corresponding to the very broad  $(\frac{3}{2}^+, \frac{5}{2}^+)$  level at 4.7 MeV.

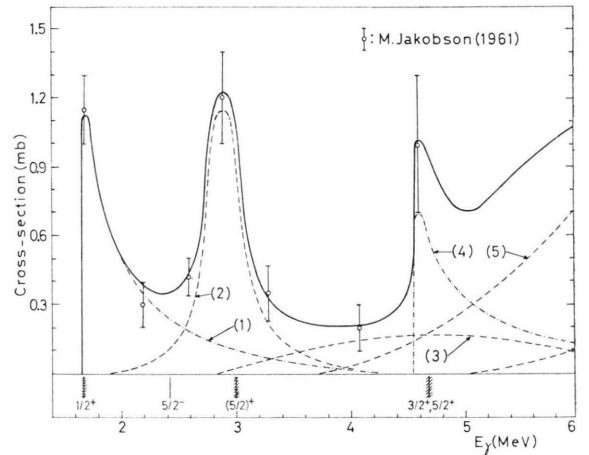


Fig. 2. Upper part: Calculated electric-dipole cross sections for the  $^9\text{Be}(\gamma, n)^8\text{Be}$  reaction. Solid line represents total photo-neutron cross sections. Dashed lines represent contributions from different reaction channels: — — — S-wave neutron cross sections, — — — D-wave neutron cross sections. The numeration of the dashed curves corresponds to bracketed numbers written in the text besides the indicated transitions. Lower part: Energy levels reproduced from Ref. <sup>9</sup>.

*The Pygmy resonance:* This very broad resonance can as seen from Fig. 3, be considered as consisting of two parts. A low energy part consisting of E1 transitions between the states

$$(l=1, L=0, J^\pi = \frac{3}{2}^-) \rightarrow (l=2, L=0, J^\pi = \frac{3}{2}^+).$$

and

$$(l=1, L=0, J^\pi = \frac{3}{2}^-) \rightarrow (l=2, L=0, J^\pi = \frac{5}{2}^+). \quad (5)$$

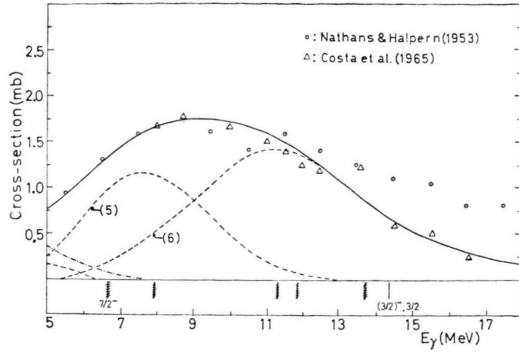


Fig. 3. Calculated electric-dipole cross sections for the  ${}^9\text{Be}(\gamma, n){}^8\text{Be}$  reaction. The symbols are the same as in Fig. 2.

and a high energy part due to E1 transitions between the following states

$$(l=1, L=2, J^\pi = \frac{3}{2}^-) \rightarrow (l=2, L=2, J^\pi = \frac{3}{2}^+).$$

and

$$(l=1, L=2, J^\pi = \frac{3}{2}^-) \rightarrow (l=2, L=2, J^\pi = \frac{5}{2}^+). \quad (6)$$

The channels with the higher spin are giving slightly higher contributions to the cross sections.

The maximum of the low energy part is seen from Fig. 3 to correspond with a broad level at 7.94 MeV of unknown spin. The high energy part can be attributed to a group of broad levels of unknown spin at 11.30 MeV, 11.82 MeV and possibly also 13.72 MeV and 14.39 MeV. The present calculations indicate that at least some of these are  $J^\pi = \frac{3}{2}^+$  and  $J^\pi = \frac{5}{2}^+$  levels.

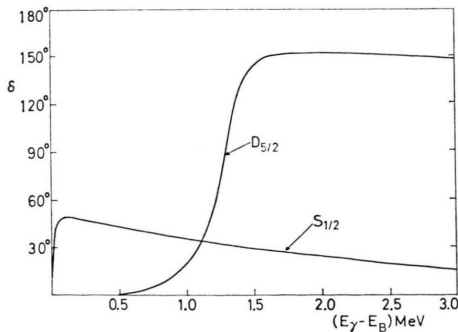


Fig. 4. S- and D-wave phase shifts calculated for neutrons scattered on  ${}^9\text{Be}$  using Saxon-Woods wavefunctions.

### 3. Conclusion

As seen from Figs. 2 and 3 there is an over-all agreement between the calculated total cross section and the experimental data in the low as well as in the intermediate energy region. This is an indication on the applicability of our model to the photodisintegration of  ${}^9\text{Be}$  in this energy range. The cross sections are, however, very sensitive to a variation of the parameter sets, and the accepted parameter values are therefore not to be considered as definite.

The calculations are revealing the importance of the excited  $2^+$  core state. Shifting the parameters  $\alpha_1$  and  $\alpha_2$  in Eq. (14) to the simple model limit ( $\alpha_1 = 1$ ,  $\alpha_2 = 0$ ) the cross sections are changed in the following way:

The 1.7 MeV and the 2.95 MeV resonances are blowing up as their channel widths are increasing.

The 4.6 MeV resonance as well as the high energy part of the Pygmy resonance vanish, as these contributions to the total cross sections are intimately connected with the excited  $2^+$  core state.

In addition to the considered E1 transitions there are, especially in the Pygmy resonance region, possibly M1 and E2 transitions to negative parity states like that at 6.66 MeV and may be others at higher energies. From the order of magnitude of such contributions relative to E1 transitions, these would cause only small corrections to the total cross section. Such transitions are possibly responsible for the small increase in the total cross section reported by Costa et al. at 13.5 MeV.

However, without more knowledge of the spin assignments of the different levels, it is not from the present model possible to give any further specifications of the cross sections.

The author wants to express his gratitude to Dr. A. AURDAL for most valuable help and to Dr. H. WITTERN for his interest and many stimulating discussions. He also acknowledges Professor Dr. K. WILDERMUTH and the members of the Institut für Theoretische Physik in Tübingen for extended hospitality. The work is sponsored by the Bundesministerium für wissenschaftliche Forschung.